Multi-Agent Control Using Coverage Over Time-Varying Domains

Xiaotian Xu* and Yancy Diaz-Mercado

Abstract

Multi-agent coverage control is used as a mechanism to influence the behavior of a group of robots by introducing time-varying domain. The coverage optimization problem is modified to adopt time-varying domains, and the proposed control law possesses an exponential convergence characteristic. Cumbrous control for many robots is simplified by deploying distribution and behavior of the robot team as a whole. In the proposed approach, the inputs to the multi-agent system, i.e., time-varying density and time-varying domain, are agnostic to the size of the system. Analytic expressions of surface and line integrals present in the control law are obtained under uniform density. The scalability of the proposed control strategy is explained and verified via numerical simulation. Experiments on real robots are used to test the proposed control law.

1 Introduction

Coverage control of multi-agent system has been drawing attention for a long time due to its wide applications, such as surveillance or exploration of an interested region. However, most of works consider these regions are static. We investigate the case that the interested areas are dynamic in this paper and extend the potential applications of coverage control of multi-agent systems. Typically, coverage control employs a group of robots to optimally cover an interested area. A classical solution to coverage problems is proposed by involving proper partitions of the domain[1, 2]. Coverage control based schemes have been previously developed for multi-agent systems, e.g., broadcast control (BC) scheme [3] and pivot-based collective coverage algorithm [4]. In [5, 6] the authors introduce a mechanism to influence the collaborative behavior between robots in coverage control by associating time-varying densities to the domain. An approach to perform coverage control on moving regions is discussed in [7]. However, the robot team is not able to maintain the centroidal Voronoi tessellation (CVT) configuration of the moving region, which will be one of the topics considered in this paper.

In this paper, the coverage control algorithm [5] is taken as a mechanism to affect the behavior of a big multi-robot team by involving time-varying domains. We define a time-varying subdomain in the workspace, and command the robots to optimally distribute in the time-varying subdomain. Under this strategy, when the subdomain moves and the shape or the scale of the subdomain changes, the robot team will act in a coordinating manner. The proposed control strategy allows the multi-objective control of multi-agent systems to be simplified into manipulating the subdomain directly, e.g., patrolling along the trajectory, and changing the size of robot group. Nevertheless, the formation of the robot team can be controlled by adopting time-varying densities within the subdomain as suggested in [6, 8].

The outline of this study is as follows. In Section 2, we state the coverage problem and recall pertinent prior work. The coverage control over time-varying domains strategy is proposed in Section 3. Analytic solutions are presented in Section 4 under the uniform density. The scalability of the proposed algorithm is presented and validated in Section 5. A robotic implementation of the proposed control scheme together with results of experiments are illustrated in Section 6. Finally, conclusions are summarized in Section 7.

---

*Authors are with the Department of Mechanical Engineering, 2181 Glenn L. Martin Hall, Building 088, University of Maryland, College Park, MD 20742, USA. Email: xxu0116@umd.edu, yancy@umd.edu.

2 Preliminaries

Coverage control will be used as a mechanism to influence the behavior of the multi-robot team, to coordinate their inter-robot motion, and manipulate their motion in the workspace. In this section, we provide some preliminary descriptions of the coverage control problem that is addressed with the modifications needed to account for time-varying domains.

2.1 The Coverage Problem

Let $p_i \in \mathcal{D} \subseteq \mathbb{R}^d$ be the position of the ith robot, $i \in \{1, \ldots, n\}$, in the domain of interest $\mathcal{D}$, i.e., the robot workspace. Further define a convex time-varying *subdomain* $\mathcal{S}(t) \subset \mathcal{D}$, such that robot i is said to lie in the subdomain at time t if $p_i(t) \in \mathcal{S}(t)$. Let $\partial \mathcal{S}(t)$ denote the boundary of the subdomain at time t, and let $q(t)$ be differentiable for almost every $q \in \partial \mathcal{S}$.

We will use the locational cost [9] as a metric of the coverage performance in the subdomain $\mathcal{S}(t)$ at time t:

$$\mathcal{H}(p(t), t) = \sum_{i=1}^{n} \int_{V_i(p(t),t)} \|p_i(t) - q\|^2 \, \phi(q, t) \, dq \tag{1}$$

where $p(t) = \left[p_1^T(t), \ldots, p_n^T(t)\right]^T$ is the configuration of the multi-robot team and $\phi : \mathcal{S}(t) \times [0, \infty) \to (0, \infty)$ is a density function that captures the relative importance of the points in the subdomain at time t, differentiable in both arguments. The subdomain is partitioned into regions of dominance, and these form a proper partition of the subdomain. We utilize a Voronoi tessellation of the domain, given by

$$V_i(p, t) = \{q \in \mathcal{S}(t) \mid \|p_i - q\| \leq \|p_j - q\| \;\; \forall j\}$$

where for ease of notation we have dropped the explicit time dependency on the configuration of the multi-robot system.

2.2 Centroidal Voronoi Tessellations

A necessary condition for the minimization of the locational cost in (1) is known to be that the agents form a centroidal Voronoi tessellation (CVT) of the domain [9], i.e.,

$$p_i(t) = c_i(p, t) \qquad \forall i$$

where we define $c_i(t) \in V_i(p, t)$ to be the center of mass of Voronoi cell i at time t, given by

$$c_i(p, t) = \frac{\int_{V_i(p,t)} q\phi(q, t) \, dq}{m_i(p, t)} \tag{2}$$

where $m_i(p, t)$ is the mass of the corresponding cell,

$$m_i(p, t) = \int_{V_i(p,t)} \phi(q, t) \, dq. \tag{3}$$

2.3 Coverage Control Law

In [5], a control law was proposed which was later shown in [6] to achieve exponential converge to a CVT in the case of time-varying densities. This control law was called TVD-C for *time-varying densities, centralized case*, given by

$$\dot{p} = \left(I - \frac{\partial c}{\partial p}\right)^{-1} \left(\kappa(c(p, t) - p) + \frac{\partial c}{\partial t}\right) \tag{4}$$

where the tuning parameter $\kappa > 0$ controls the exponential convergence rate, and

$$c(p, t) = \left[c_1(p, t)^T, \ldots, c_n(p, t)^T\right]^T.$$

When many agents are used, the control law called TVD-D$_1$, which stands for *time varying densities, decentralized case with 1-hop adjacency information*, bypasses difficulties with computing the matrix inverse in (4) by approximating it with the truncated Neumann series,

$$\dot{p} = \left(I + \frac{\partial c}{\partial p} \right) \left(\kappa(c(p,t) - p) + \frac{\partial c}{\partial t} \right). \tag{5}$$

The matrix $\frac{\partial c}{\partial p}$ in (4) and (5) is a block matrix that possess the sparsity structure of the Delaunay graph associated with the Voronoi tessellation [6]. The ij^{th} block is given by

$$\left[\frac{\partial c}{\partial p} \right]_{ij} = \frac{\partial c_i}{\partial p_j} = -\frac{\int_{\partial V_{ij}(p,t)} (q - c_i)(q - p_j)^T \phi(q,t)\, dq}{m_i(p,t)\|p_i - p_j\|} \tag{6}$$

when $i \neq j$, and

$$\left[\frac{\partial c}{\partial p} \right]_{ii} = \frac{\partial c_i}{\partial p_i} = \sum_{j \in \mathcal{N}_{V_i}} \frac{\int_{\partial V_{ij}(p,t)} (q - c_i)(q - p_i)^T \phi(q,t)\, dq}{m_i(p,t)\|p_i - p_j\|} \tag{7}$$

where $\partial V_{ij} = V_i \cap V_j$, and $\mathcal{N}_{V_i}$ is the Delaunay graph neighbor set of agent i. These are $(d-1)$-dimensional integrals (e.g., line integrals if $\mathcal{D} \subseteq \mathbb{R}^2$), and are zero if $\partial V_{ij} = \emptyset$ (i.e., two cells are not adjacent), or if the shared boundary has zero $(d-1)$-dimensional measure (e.g., points in 2D).

Assuming that the domain of interest is static, the partial $\frac{\partial c}{\partial t}$ in (4) is given by $\frac{\partial c}{\partial t} = \left[\frac{\partial c_1}{\partial t}^T, \ldots, \frac{\partial c_n}{\partial t}^T \right]^T$, where

$$\frac{\partial c_i}{\partial t} = \frac{\int_{V_i(p,t)} (q - c_i)\frac{\partial \phi}{\partial t}\, dq}{m_i(p,t)}. \tag{8}$$

Although the control law in (4) was derived with consideration to time-varying densities over static domains, the proof of exponential convergence in [6] is still valid when the domain of interest is time-varying with almost everywhere differentiable boundary, as long as $p_i(t_0) \in \mathcal{S}(t_0)\ \forall i$. However, additional terms are needed in (8) to capture the evolution of the subdomain. In the following sections, we will derive the needed terms such that (4) is able to provide exponential convergence to a CVT configuration, even when the subdomain of interest is time-varying.

3 Time-Varying Domains

In order to retain the exponential convergence to a CVT property of control law (4), we will need to add additional terms in (8) to capture the evolution of the time-varying domain. For the subsequent analysis, it is assumed that $\frac{dq}{dt}$ exists and is known for almost every $q \in \partial \mathcal{S}(t)$.

Note that the center of mass integrals in (2) are time dependent in both the integral kernel and the domain of integration. Thus, Leibniz integral rule is needed.

Lemma 1 (Leibniz Integral Rule[10])**.** *Let $\Omega(p,t)$ be a region that depends smoothly on t and that has a well-defined boundary $\partial\Omega(p,t)$. If $F(p,t) = \int_{\Omega(p,t)} f(p,t,q)\, dq$ for differentiable f, then*

$$\frac{\partial F}{\partial t} = \int_{\Omega(p,t)} \frac{\partial f}{\partial t}\, dq + \int_{\partial\Omega(p,t)} f(p,t,q) \frac{\partial q}{\partial t}^T \hat{n}(q)\, dq$$

where $\hat{n}(q)$ is the unit outward normal for $q \in \partial\Omega(p,t)$.

Application of Lemma 1 to (2) yields the following result.

Proposition 1 (Time-Varying Domains)**.** *Let $\mathcal{S}(t)$ be the convex subdomain to be covered with boundary $\partial\mathcal{S}(t)$. Assume that $\frac{dq}{dt}$ exists and is known for almost every $q \in \partial\mathcal{S}(t)$. Let $\partial\mathcal{S}_i(p,t) = \partial\mathcal{S}(t) \cap V_i(p,t)$. Then the partial derivative $\frac{\partial c_i}{\partial t}$, which captures the time evolution of the center of mass of the ith Voronoi cell due to the motion of the subdomain and the change in density function, is given by*

$$\frac{\partial c_i}{\partial t} = \frac{1}{m_i(p,t)} \int_{V_i(p,t)} (q - c_i)\frac{\partial \phi}{\partial t}\, dq + \frac{1}{m_i(p,t)} \int_{\partial\mathcal{S}_i(p,t)} (q - c_i)\phi(q,t)\frac{dq}{dt}^T \hat{n}\, dq. \tag{9}$$

3

Proof. By the product rule, we find

$$\frac{\partial c_i}{\partial t} = \frac{\frac{\partial}{\partial t}\left(\int_{V_i(p,t)} q\phi(q,t)\,dq\right)}{m_i(p,t)} - \frac{c_i(p,t)}{m_i(p,t)}\frac{\partial m_i}{\partial t}.$$

Both terms now contain derivatives of integrals with time-varying integral kernels and domains. Applying Leibniz integral rule to the first term yields

$$\frac{\partial}{\partial t}\left(\int_{V_i(p,t)} q\phi(q,t)\,dq\right) = \int_{V_i(p,t)} q\frac{\partial\phi}{\partial t}\,dq + \int_{\partial V_i(p,t)} q\phi(q,t)\frac{\partial q}{\partial t}^T \hat{n}\,dq$$

Then the latter integral can be split into two terms: for $q \in \partial \mathcal{S}_i(p,t)$, and for $q \in \partial V_i(p,t)\backslash\partial\mathcal{S}_i(p,t)$. Note that only the points on the boundary of the subdomain change explicitly with time, i.e., since $\frac{\partial q}{\partial t} = 0$ for almost every point $q \notin \partial\mathcal{S}_i(p,t)$ we get

$$\frac{\partial}{\partial t}\left(\int_{V_i(p,t)} q\phi(q,t)\,dq\right) = \int_{V_i(p,t)} q\frac{\partial\phi}{\partial t}\,dq + \int_{\partial\mathcal{S}_i(p,t)} q\phi(q,t)\frac{dq}{dt}^T \hat{n}\,dq.$$

Similarly, for $\frac{\partial m_i}{\partial t}$ we find

$$\frac{\partial m_i}{\partial t} = \int_{V_i(p,t)} \frac{\partial\phi}{\partial t}\,dq + \int_{\partial\mathcal{S}_i(p,t)} \phi(q,t)\frac{dq}{dt}^T \hat{n}\,dq.$$

Collecting like terms, we get

$$\frac{\partial c_i}{\partial t} = \frac{\int_{V_i(p,t)}(q - c_i)\frac{\partial\phi}{\partial t}\,dq}{m_i(p,t)} + \frac{\int_{\partial\mathcal{S}_i(p,t)}(q - c_i)\phi(q,t)\frac{dq}{dt}^T \hat{n}\,dq}{m_i(p,t)}$$

as was to be shown. ∎

Corollary 1 (Exponential Convergence). *The control law in (4) with updated partial derivative as in Proposition 1 yields exponential convergence to a CVT with exponential decay rate controlled by $\kappa > 0$ over smoothly time-varying domains and densities, as long as $p_i(t_0) \in \mathcal{S}(t_0)\ \forall i$.*

Proof. Same as in [6]. ∎

Proposition 1 introduces a new term in the computation of $\frac{\partial c_i}{\partial t}$ when compared to (8), which allows us to explicitly take into account the evolution of the subdomain. This additional term can serve as an exogenous input to the multi-robot team to control their collective position and scale, while the density function can be chosen to provide the desired shape in multi-robot team formations, as suggested in [11]. These choices of inputs possess the advantages of being flexible with respect to the size of the system, and as well as being identity-agnostic, so that the input may be chosen without the need of performing assignments of roles, such as is needed in leader-follower schemes.

In the next section, we explore the coverage problem over uniform densities in convex 2-polytope subdomains, and analytical expressions are found for the terms in (4) and (5).

4 Coverage over Convex 2D-Polytopes with Uniform Density

We now focus on the class of coverage problems where the subdomain is a convex polytope in $\mathbb{R}^2$ with N vertices using uniform density, i.e., with $\phi(q,t) = 1$ for all $q \in \mathcal{S}(t)$ and $t \geq 0$. As an immediate consequence of this, the first term in expression provided in Proposition 1 becomes zero. For this class of problems, we will further see that we can find analytical expressions in terms of time, neighboring agent positions and boundary conditions in that agent's Voronoi cell. The control law can be computed solely on local neighbor information and broadcasted domain information. We begin by considering the vertices of a Voronoi cell.

4.1 Vertices of the Voronoi Cell

Assuming that agent i has h' neighbors, the ith Voronoi cell will be a convex 2-polytope with at least $h'-1$ vertices. To account for vertices due to the intersection of the Voronoi cell with the the subdomain boundary, we will assume the Voronoi cell consists of $M \geq h'-1$ vertices. We will denote the vertex due to neighbors j and k (which can be determined by employing a Delaunay triangulation [12]) as V_{ijk}. The vertex location V_{ijk} is given by the circumcenter of the triangle formed by connecting the position of these three agents p_i, p_j and p_k, and can be found analytically in terms of these [13, 14]. We present the equation below for the sake of completion,

$$V_{ijk} = \frac{1}{2}\frac{\alpha_i p_i + \alpha_j p_j + \alpha_k p_k}{||p_{ij}||^2 ||p_{jk}||^2 - (p_{ij}^T p_{jk})^2}$$

where the agents are assumed to be oriented in a counterclockwise order, where $p_{ab} = p_b - p_a$, and where

$$\alpha_i = ||p_{jk}||^2 p_{ij}^T p_{ik}, \alpha_j = ||p_{ik}||^2 p_{ij}^T p_{kj}, \alpha_k = ||p_{ij}||^2 p_{ik}^T p_{jk}.$$

Denote $V_{i\mathcal{S}\ell}$ to be the ℓth vertex of the ith Voronoi cell that is on the subdomain boundary, where without loss of generality these are assumed to be ordered counterclockwise. These may be domain polytope vertices, or may be vertices due to the intersection of the Voronoi cell with the subdomain. As the former vertices are assumed to be known, we provide an analytical expression for the latter.

Any point q on a face of the subdomain may be expressed using the vertices that define the face via the parameterization $q = L_\ell(\tau) = \partial\mathcal{S}^\ell + (\partial\mathcal{S}^{(\ell+1)} - \partial\mathcal{S}^\ell)\tau$ for certain $\tau \in [0, 1]$, where without loss of generality the vertices of the subdomain $\partial\mathcal{S}^\ell$ are assumed to be ordered counterclockwise, and where $\partial\mathcal{S}^{N+1} = \partial\mathcal{S}^1$. Let any point $q \in \partial V_{ij}$, the interior Voronoi face due to two agents i and j that intersects polytope edge L_ℓ, be given by $q = R_{ij}(s) = \frac{1}{2}(p_i + p_j) + t_{ij}s$ for certain $s \in \mathbb{R}$, where $t_{ij} = S(p_j - p_i)$ with $S = \begin{bmatrix} 0 & -1 \\ 1 & 0 \end{bmatrix}$ being a skew symmetric rotation matrix. The sough after vertex $V_{i\mathcal{S}j}$ is given by

$$V_{i\mathcal{S}j} = \partial\mathcal{S}^\ell + \left(\partial\mathcal{S}^{(\ell+1)} - \partial\mathcal{S}^\ell\right)\tau^*$$

which exists if

$$\tau^* = \frac{\left(\frac{1}{2}(p_i + p_j) - \partial\mathcal{S}^\ell\right)}{\left(\partial\mathcal{S}^{(\ell+1)} - \partial\mathcal{S}^\ell\right)^T (p_j - p_i)} \in [0, 1]$$

found from solving for τ in $L_\ell(\tau) = R_{ij}(s)$.

The mass and center of mass can now be computed analytically in terms of the vertices of the Voronoi cell.

4.2 Mass and Center of Mass of a Voronoi Cell

For convenience, denote the vertices of the ith Voronoi cell as $V_{ij}(p, t)$, $j \in \{1, \ldots, M\}$, which are assumed without loss of generality to be ordered counterclockwise. Then the mass and center of mass may be computed as [14]

$$m_i(p, t) = \frac{1}{2}\sum_{j=1}^{M-1} V_{i(j+1)}^T S V_{ij}$$

$$c_i(p, t) = \frac{1}{6m_i(p, t)}\sum_{j=1}^{N-1} \left(V_{i(j+1)} + V_{ij}\right)\left(V_{i(j+1)}^T S V_{ij}\right).$$

4.3 Partial Derivatives of a Centroid

For a convex 2-polytope subdomain, every Voronoi cell is also a convex 2-polytope, and the boundary integrals in (6), (7), and (9) may be solved along each face analytically by using the parametric line integral as in the following lemma.

5

Lemma 2 (Parametric Line Integral). *Let the line integral of $f(q)$ along L be denoted by $\int_L f(q)dq$ where the point $q = [q_1, q_2]^T$ can be parameterized such that if $q_1 = h(\tau)$ and $q_2 = g(\tau)$ for some $\tau \in [t_0, t_1]$, then*

$$\int_L f(q)dq = \int_{t_0}^{t_1} f([h(\tau), g(\tau)]^T) \|q'(\tau)\| dt$$

where $\|q'(\tau)\| = \sqrt{(\frac{dh}{d\tau})^2 + (\frac{dg}{d\tau})^2}$.

Let that $\partial \mathcal{S}_i(p, t) = \partial \mathcal{S}(t) \cap V_i(p, t) = \bigcup_j \partial \mathcal{S}_i^j$, where $\partial \mathcal{S}_i^j$ is the jth Voronoi cell face shared with the subdomain boundary. Each of the $\partial \mathcal{S}_i^j$ is a straight line, connected by two Voronoi cell vertices v_1^j and v_2^j. By linearity of the integral, the partial derivative (9) may be computed as

$$\frac{\partial c_i}{\partial t} = \sum_j \frac{\nu_j(t)}{m_i} \int_{\partial S_i^j} (q - c_i) \, dq$$

where $\nu_j(t)$ is the velocity of the points in the boundary ∂S_i^j, assumed to be the same for every point, projected in the unit outward direction (i.e., $\nu_j(t) = \pm \frac{dq}{dt}^T S \frac{v_2^j - v_1^j}{\|v_2^j - v_1^j\|} \forall q \in \partial S_i^j$ depending on the orientation of the vertices).

Lemma 3 (Analytic Partial Derivatives).

Under uniform density and a convex 2-polytope subdomain with $\partial \mathcal{S}_i^j = \overline{v_1^j v_2^j}$, (9) can be expressed as

$$\frac{\partial c_i}{\partial t} = \sum_j \frac{\nu_j(t)}{2m_i} \left(\left(v_2^j - c_i \right) + \left(v_1^j - c_i \right) \right) \|v_2^j - v_1^j\|$$

and for $\partial V_{ij} = \overline{v_1^j v_2^j}$, (6) may be expressed as

$$\frac{\partial c_i}{\partial p_j} = -\frac{\|v_2^j - v_1^j\|}{m_i \|p_i - p_j\|} \Big[\left(v_1^j - c_i \right) \left(v_1^j - p_j \right)^T + \frac{1}{2} \left((v_1^j - c_i)(v_2^j - v_1^j)^T + (v_2^j - v_1^j)(v_1^j - p_j)^T \right)$$
$$+ \frac{1}{3} \left(v_2^j - v_1^j \right) \left(v_2^j - v_1^j \right)^T \Big].$$

Proof. Assume the following parameterization of the points $q \in \partial S_i^j = \overline{v_1^j v_2^j}$,

$$q(\tau) = v_1^j (1 - \tau) + v_2^j \tau, \ \ \tau \in [0, 1].$$

It follows that $q' = (v_2^j - v_1^j)$ for all τ, and consequently $dq = \|v_2^j - v_1^j\| d\tau$. Applying Lemma 2 to the integral in (9),

$$\frac{\partial c_i}{\partial t} = \sum_j \frac{\nu_j(t)}{m_i} \int_0^1 \left(v_1^j (1 - \tau) + v_2^j \tau - c_i \right) \|v_2^j - v_1^j\| d\tau.$$

The result follows from expanding and integrating the terms. A similar process can be applied to (6) by instead using the vertices that make up the boundary for ∂V_{ij} in the parameterization. ∎

5   Scalability of the Algorithm

In this section, we will argue that the proposed algorithm is scalable for a large group of robots (e.g., robot swarms). As a well-known fact in the field of computational geometry, the number of edges meeting at a vertex in the Voronoi diagram is not less than three, and each edge connects two vertices; it follows Euler's relation that the average number of edges of a Voronoi cell equals six[15, 16]. This fact is the key for our algorithm's significantly reduced computational cost.

Table 1: Number of agents (out of 100) categorized by their neighbor sets $\mathcal{N}_i$ (i.e., number of neighbors).

Size of $\mathcal{N}_i$	2	3	4	5	6	7
Simulation	Number of Agents					
Trial 1	4	1	31	10	47	7
Trial 2	1	4	29	9	50	7
Trial 3	2	3	28	9	52	6
Trial 4	3	4	28	8	51	6
Trial 5	3	3	27	9	52	6
Average	2.6	3	28.6	9	50.4	6.4

5.1 Complexity Analysis of the Algorithm

Here we analyze the time complexity of the proposed algorithm for a single agent p_i.

1. There are many well-studied algorithms to construct Voronoi diagrams, such as the Incremental Insertion Method and the Divide and Conquer Method[15]. The quaternary incremental algorithm builds the Voronoi diagram for n seeds with average complexity $O(n)$ despite its worst-case complexity $O(n^2)$, and the Divide and Conquer Method has an average and worst-case complexity $O(n \log n)$[16]. In our algorithm, agents only require the density and boundary information within their own Voronoi cells (which can be computed in a distributed way [14]) and their Delaunay neighbor positions to compute the quantities in (4). As described in [5], the matrix inverse in TVD-C can be approximated using the truncated Neumann series expansion so that an agent only use as much information about the multi-robot team as it has access to. For one agent in our algorithm, only a partial Voronoi diagram, which is generated by the agent itself, its neighbors ($|\mathcal{N}_i| = 6$ on average), and its neighbors' neighbors (to enclose the Voronoi cells of $\mathcal{N}_i$, a total of 12 on average) is needed instead of the overall Voronoi diagram. Thus, the time complexity becomes $O\left(\left|\bigcup_{j \in \mathcal{N}_i} \mathcal{N}_j \cup \mathcal{N}_i\right|\right)$, which is on average constant time, by using the quaternary incremental algorithm.

2. We can obtain necessary information for $\frac{\partial c}{\partial p}$ in the control law (i.e., masses m_i and m_j, centroids c_i and c_j of Voronoi cell V_i and $V_j \in \mathcal{N}_i$) in constant time thanks to analytic expressions derived in previous section. The complexity becomes $O(1)$ on average in light of the fact of average number of neighbors is independent of the size of the robot team.

3. The complexity of computing $\frac{\partial c_i}{\partial t}$ is determined by the number of edges of its Voronoi cell ($O(M)$). Similarly to the previous cases, as the number of edges depends on the number of neighbors, the complexity is constant time on average.

4. Given the above terms, the control law for agent p_i can be calculated with time complexity $O(1)$.

5.2 Validation of Scalability

We show the asymptotic nature of the average number of neighbors and the efficiency of the control law for a large group of robots via numerical simulations. The simulation of the proposed control strategy was run for five trials using 100 robots with random initial configurations, and the outcomes are collected in Table 1. Around fifty percent of agents have 6 neighbors in the simulations. The majority of the remaining agents actually had less, with only about 7% having no more than seven neighbors. This percentage increased with the size of the swarm.

Moreover, simulations of the proposed control law with and without term $\frac{\partial c}{\partial t}$ are conducted. The simulation is shown in Fig. 1i, where a team of 100 robots is performing coverage of a subdomain which is tracking a circular trajectory. The instantaneous aggregated CVT error $e_a(t) = \|p(t) - c(p, t)\|$ of the proposed control strategy with and without the term $\frac{\partial c}{\partial t}$ is shown in Fig. 1ii. As we can tell from the results, the steady state
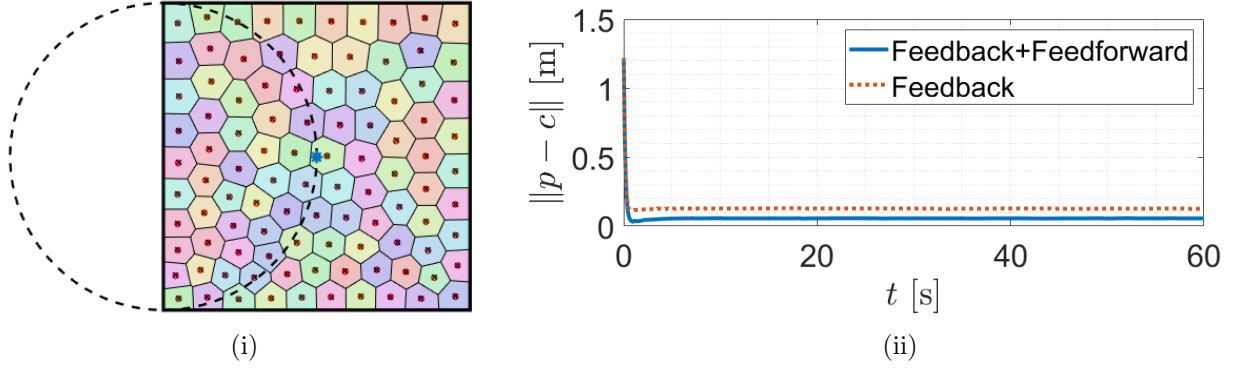
(i)   (ii)

Figure 1: Simulation of a group of 100 single-integrator robots (i); the center of subdomain (asterisk) moves along the circular trajectory (dash line) in counterclockwise fashion. Results of the simulation of the control law with and without the additional feedforward term $\frac{\partial c}{\partial t}$ (ii).

mean values of the simulation with and without $\frac{\partial c}{\partial t}$ are 0.0562 m and 0.1248 m respectively. The aggregated CVT error 0.0562 m for 100 robots (i.e., 0.000562 m on average for each robot) suggests that the proposed control law converges to a CVT. The $\frac{\partial c}{\partial t}$ term improves the error performance by 54.97% in this scenario with a large group of agents. The error is not exactly zero because the distributed form of the control law (5) was used, which does not perform feedforward on every agent in the team. Thus, the agents on the boundary can immediately follow the motion of subdomain as they have direct access to the boundary conditions (i.e., whose Voronoi cell boundaries have overlapped edges with subdomain's boundaries), but the agents on the interior must wait for the boundary conditions to propagate through feedback.
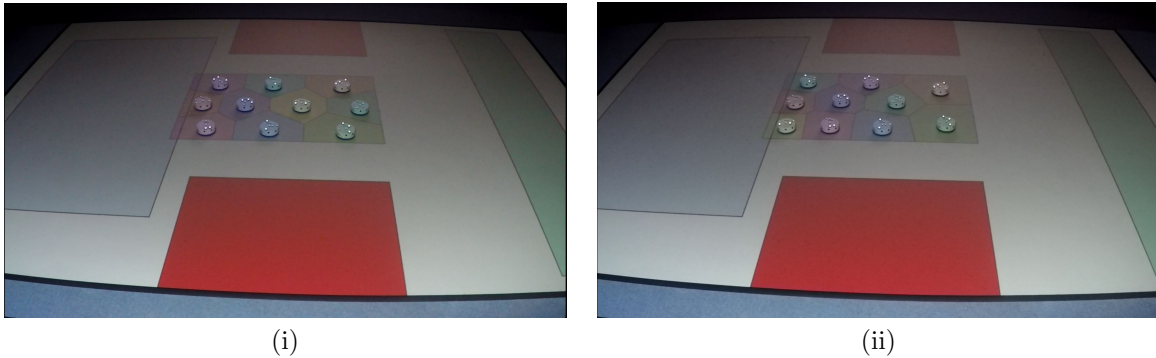
6   Multi-Robot Implementation

(i)   (ii)

Figure 2: Multi-robot implementation of control law with (i) and without (ii) term $\frac{\partial c}{\partial t}$. 10 robots travel from left end of workspace (blue box) towards the right end (green box) while avoiding the obstacles (red boxes). The subdomain translates and scales over time. An overhead projector is used to visualize the subdomain, goal location and obstacles in real time.

In section 4, the coverage control laws (4) and (5) are modified to account for time-variations in the subdomain and the terms needed for the equations are provided analytically in the case of uniform coverage on a convex 2-polytope domain. The results were simulated on a large team of robots in Section 5. In this section, we implement the proposed control strategy on a group of real mobile robots. The experiments are carried out on a workstation with *Intel(R) Xeon(R) W-2125 processor*, and the algorithms are implemented in *MATLAB*. The multi-robot team consists of 10 *Khepera IV* differential-drive mobile robots. A motion capture system consisting of 8 *Vicon Vantage V8* cameras are used to provide real-time position information
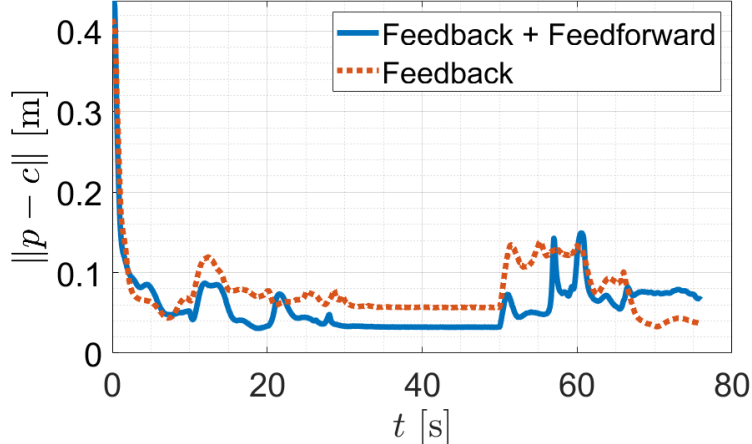
Figure 3: Results of experiments. Profiles of aggregated error from optimal configuration with and without term $\frac{\partial c}{\partial t}$ are indicated by blue solid line and red dot line

of the multi-robot team, and an overhead projector is used to visualize a virtual environment and Voronoi tessellation. The robot workspace is defined to be a 5.182 m × 3.658 m (17 feet × 12 feet) rectangular area.

6.1 Experiment Description

An experiment is carried out to validate the proposed control strategy with a rectangular subdomain $\partial \mathcal{S}(t) = [x_{min}(t), x_{max}(t)] \times [y_{min}(t), y_{max}(t)]$ with uniform density. In the experiment, we synthesize control laws for the different agents by driving the coverage domain for a group of robots to achieve a motion plan. The experiment is shown in Fig. 2. To achieve the task, the subdomain simultaneously translates and scales to go through the narrower passage and avoid the obstacles. The velocities for the subdomain boundaries are defined as piece-wise constants to achieve the desired scaling and translation. The metric used to determine performance of the proposed control strategy on the real robots is same as that in simulation. The control law (5) and analytic expressions presented in Section 4 are used for the experiment with a control gain $\kappa = 2$.

As mentioned in Corollary 1, the aggregated error e_a is expected to decay exponentially to zero under control law TVD-C (almost exponential convergence under control law TVD-D$_1$), up to the error introduced by the mapping of the control law to the differential-drive motion of the robots, wheel saturations, and delays. For comparison, the experiment is executed with and without the term $\frac{\partial c}{\partial t}$, to evaluate the contribution by the inclusion of the term.

6.2 Experimental Results

From Fig. 2, we can tell the difference between performances with and without $\frac{\partial c}{\partial t}$. The robots form and maintain an almost symmetric configuration with $\frac{\partial c}{\partial t}$ (Fig. 2i) while the robots lag behind the motion of subdomain (Fig. 2ii) and could fail to catch up if the subdomain moves faster. Moreover, the profiles of $\|p(t) - c(p, t)\|$ are plotted in Fig. 3 for the experiments of implementing the control law with the inclusion of the $\frac{\partial c}{\partial t}$ term and the absence of it, and they are shown as blue solid line and red dot line respectively. The aggregated error e_a greatly decreases at first, as expected due to the exponential convergence. As the agents approach their CVT configuration, delays, saturations, and errors in mapping velocities to differential-drive introduce small disturbances that result in variations along a small constant value. The mean of the steady-state values of the metric are 0.0323 m (i.e., 0.0032 m per robot — well within the footprint of the robots which are 0.14 m in diameter) and 0.057 m for with and without the inclusion of $\frac{\partial c}{\partial t}$. There is a noticeable improvement in e_a of nearly 43.3% due to the presence of the feedforward term.

7 Conclusion

An innovative control scheme is developed of synthesizing multi-agent controllers via coverage control on time-varying domains. The approach offers a capability of controlling the behavior of multi-agent systems by simply manipulating the domain to be covered, and it has the advantage of being agnostic to the size of the system. Analytic solutions for the uniform density case is obtained, and scalability of the approach is demonstrated. The feasibility of proposed control strategy is validated in simulation for a large number of agents and experimentally on a team of real differential-drive wheeled robots.

References

[1] Stuart Lloyd. Least squares quantization in pcm. *IEEE transactions on information theory*, 28(2):129–137, 1982.

[2] Jorge Cortes, Sonia Martinez, and Francesco Bullo. Spatially-distributed coverage optimization and control with limited-range interactions. *ESAIM: Control, Optimisation and Calculus of Variations*, 11(4):691–719, 2005.

[3] Shalini Darmaraju, Md Abdus Samad Kamal, Madhavan Shanmugavel, and Chee Pin Tan. Coverage control of a mobile multi-agent serving system in dynamical environment. In *2018 Joint 7th International Conference on Informatics, Electronics & Vision (ICIEV) and 2018 2nd International Conference on Imaging, Vision & Pattern Recognition (icIVPR)*, pages 508–513. IEEE, 2018.

[4] Shaocheng Luo, Jun Han Bae, and Byung Cheol Min. Pivot-based collective coverage control with a multi-robot team. In *2018 IEEE International Conference on Robotics and Biomimetics (ROBIO)*, pages 2367–2372. IEEE, 2018.

[5] S. G. Lee, Y. Diaz-Mercado, and M. Egerstedt. Multirobot control using time-varying density functions. *IEEE Transactions on Robotics*, 31(2):489–493, April 2015.

[6] Y. Diaz-Mercado, S. G. Lee, and M. Egerstedt. Human-swarm interactions via coverage of time-varying densities. In *Trends in Control and Decision-Making for Human–Robot Collaboration Systems*, chapter 15, pages 357–385. Springer, Cham, Switzerland, 2017.

[7] Sora Nishigaki, Kenta Hoshino, and Jun Yoneyama. Coverage control in moving regions with unmanned aerial vehicles. In *2019 IEEE/SICE International Symposium on System Integration (SII)*, pages 301–306. IEEE, 2019.

[8] Xiaotian Xu and Yancy Diaz-Mercado. Multi-robot control using coverage over time-varying domains extended abstract. In *The 2nd International Symposium on Multi-Robot and Multi-Agent Systems (MRS2019)*. IEEE, In Press.

[9] J. Cortes, S. Martinez, T. Karatas, and F. Bullo. Coverage control for mobile sensing networks: variations on a theme. In *Mediterranean Conference on Control and Automation*, 2002.

[10] Qiang Du, Vance Faber, and Max Gunzburger. Centroidal voronoi tessellations: Applications and algorithms. *SIAM review*, 41(4):637–676, 1999.

[11] Y. Diaz-Mercado, S. G. Lee, and M. Egerstedt. Distributed dynamic density coverage for human-swarm interactions. In *2015 American Control Conference (ACC)*, pages 353–358, July 2015.

[12] Der Tsai Lee and Bruce J Schachter. Two algorithms for constructing a delaunay triangulation. *International Journal of Computer & Information Sciences*, 9(3):219–242, 1980.

[13] Dan Pedoe. *Circles: a mathematical view.* Cambridge University Press, 1995.

[14] J. Cortes, S. Martinez, T. Karatas, and F. Bullo. Coverage control for mobile sensing networks. *IEEE Transactions on Robotics and Automation*, 20(2):243–255, April 2004.

[15] Franz Aurenhammer. Voronoi diagrams—a survey of a fundamental geometric data structure. *ACM Computing Surveys (CSUR)*, 23(3):345–405, 1991.

[16] Takao Ohya, Masao Iri, and Kazuo Murota. Improvements of the incremental method for the voronoi diagram with computational comparison of various algorithms. *Journal of the Operations Research Society of Japan*, 27(4):306–337, 1984.